A New Model for Blood Cancer Classification Based on Deep Learning Techniques

Hagar Mohamed[1], Fahad Kamal Elsheref [2], Shrouk Reda Kamal[3]
Information System Department-Faculty of Computers and Artificial Intelligence, Beni-Suef University, Beni-Suef, Egypt[1, 2]
Information System Department-Faculty of Computer Science, Nahda University, Beni-Suef, Egypt[3]

***Abstract*—Artificial intelligence and deep learning algorithms have become essential fields in medical science. These algorithms help doctors detect diseases early, reduce the incidence of errors, and decrease the time required for disease diagnosis, thereby saving human lives. Deep learning models are widely used in Computer-Aided Diagnosis Systems (CAD) for the classification of various diseases, including blood cancer. Early diagnosis of blood cancer is crucial for effective treatment and saving patients' lives. Therefore, this study developed two distinct models to classify eight types of blood cancer. These types include follicular lymphoma (FL), mantle cell lymphoma (MCL), chronic lymphocytic leukemia (CLL), acute myeloid leukemia (AML), and the subtypes of acute lymphoblastic leukemia (ALL) known as early pre-B, pre-B, pro-B ALL, and benign. AML and ALL are specific classifications for human leukemia cancer, while FL, MCL, and CLL are specific classifications for lymphoma. Both models consist of different phases, including data collection, preprocessing, feature extraction techniques, and the classification process. The techniques applied in these phases are the same in both proposed models, except for the classification phase. The first model utilizes the VGG16 architecture, while the second model utilizes DenseNet-121. The results indicated that DenseNet-121 achieved a lower accuracy compared to VGG16. VGG16 exhibited excellent results, achieving an accuracy of 98.2% when classifying the eight classes. This outcome suggests that VGG16 is the most effective classifier for the utilized dataset.**

Keywords*—Deep learning; convolutional neural networks (CNNs); leukemia; lymphoma; computer-aided diagnosis systems (CAD)

I. Introduction

According to a report by the World Health Organization (WHO), approximately 1 in 6 deaths worldwide is caused by cancer, making it the second leading cause of death globally. Among the various types of cancer, blood cancer holds significant prominence. It accounts for approximately 9% of all cancers and is now ranked as the fourth most common cancer in both men and women worldwide [1, 2]. As a result, researchers have shifted their focus towards applying artificial intelligence techniques to develop models that can assist in addressing this issue in the medical field. In the following section, we will provide a detailed description of the most prevalent types of blood cancer.

A. Leukemia

Leukemia is a type of cancer that affects the blood cells and can occur in individuals of all ages, including children and adults [3]. It is characterized by an abnormal proliferation of immature blood cells in the bone marrow, which leads to the replacement of healthy blood cells. In leukemia, a genetic mutation takes place in an immature blood cell, causing it to transform into a cancerous cell. These malignant cells do not function properly and multiply at a faster rate compared to normal cells, while having a shorter lifespan. Consequently, the presence of cancerous cells in the bone marrow displaces the healthy blood cells [4].

Leukemia can be categorized into two main types based on the rate of malignant cell growth. If the malignant cells grow rapidly, it is classified as acute leukemia, whereas if they grow slowly, it is classified as chronic leukemia [1]. As a result, there are four primary types of leukemia: Acute Myeloid Leukemia (AML), Acute Lymphoblastic Leukemia (ALL), Chronic Myeloid Leukemia (CML), and Chronic Lymphocytic Leukemia (CLL) [5].

- Acute Myeloid Leukemia: It is the most common type of acute leukemia. It occurs when the bone marrow produces abnormal blasts and immature white blood cells (WBCs). In some cases, it may also lead to the production of abnormal red blood cells (RBCs) and platelets. The symptoms of early-stage AML may resemble those of a common cold or other illnesses [6].
- Acute Lymphoblastic Leukemia: It is a type of cancer that primarily affects white blood cells and is commonly found in children. It is characterized by the uncontrolled growth and excessive production of immature white blood cells in the bone marrow. The symptoms of ALL, which include fatigue, weakness, and joint and bone pain, can resemble those of the flu and other common illnesses, making the diagnosis challenging. ALL is further classified into three subtypes: Early Pre-B, Pre-B, and Pro-B ALL[7, 8].
- Chronic Myeloid Leukemia (CML): It is a type of cancer that primarily affects white blood cells. In individuals with CML, there is uncontrolled growth of immature white blood cells, known as blast cells, in the body [4].
- Chronic Lymphocytic Leukemia: it is a haematological disease that affects B lymphocytes or B cells. It is more prevalent in adults and rare in children. CLL symptoms include weight loss, fever, sleep sweats, and frequent infection[6].

B. Lymphoma

Lymphoma is a type of blood cancer that occurs due to the abnormal development of white blood cells called lymphocytes. Lymphocytes are specialized cells that circulate throughout the body via the blood and lymphatic systems, playing a crucial role in the immune response to prevent infections [9]. Lymphoma is characterized by the clonal proliferation of malignant lymphocytes, which can be either T cells or B cells. The diagnosis of different types of lymphoma is typically based on the growth pattern and cytological features of the abnormal cells observed under light microscopy using Hematoxylin and Eosin-stained tissue samples. Lymphoma is classified into three main subtypes: follicular lymphoma (FL), mantle cell lymphoma, and Chronic Lymphocytic Leukemia (CLL) [10].

As mentioned in the previous section, the most prevalent types of blood cancer include FL, MCL, CLL, AML, and ALL, which encompass Early Pre-B, Pre-B, Pro-B ALL, and benign subtypes. The objective of this study is to develop a classification model for accurately categorizing images into these different disease categories.

Blood cancer can be detected through manual counting using a heamatological analyzer, which involves the classification of cells based on their morphological characteristics. However, this method is often time-consuming, labor-intensive, and expensive. Moreover, manual analysis may yield inaccurate results in terms of leukocyte counts and classification. In order to address these challenges [9, 11], researchers have developed Computer-Aided Diagnosis (CAD) systems that utilize deep learning techniques to assist physicians in accurately identifying leukemia.

Deep learning algorithms have gained significant popularity in Computer-Aided Diagnosis (CAD) systems. Among these algorithms, the convolutional neural network (CNN) is one of the most widely used approaches. CNN consists of three main layers: the Convolutional Layer, the Pooling Layer, and the Fully Connected Layer. Illustrated in Fig. 1, a CNN can learn hierarchical representations of data by extracting more general features in the initial convolutional layers and progressively capturing more specific features in the subsequent layers. The effectiveness of CNNs in medical diagnosis has been well-established [4, 12].

This study makes several contributions to the field of blood cancer diagnosis. Firstly, an image augmentation technique is applied as a preprocessing step to enhance the quality of blood cancer images. Secondly, a classification method using two different CNN architectures is employed to distinguish between eight different classes of blood cancer that have not been used before. The performance of the model is also thoroughly analyzed and compared with existing state-of-the-art methods. Finally, mixed datasets are utilized to improve the accuracy of blood cancer classification.

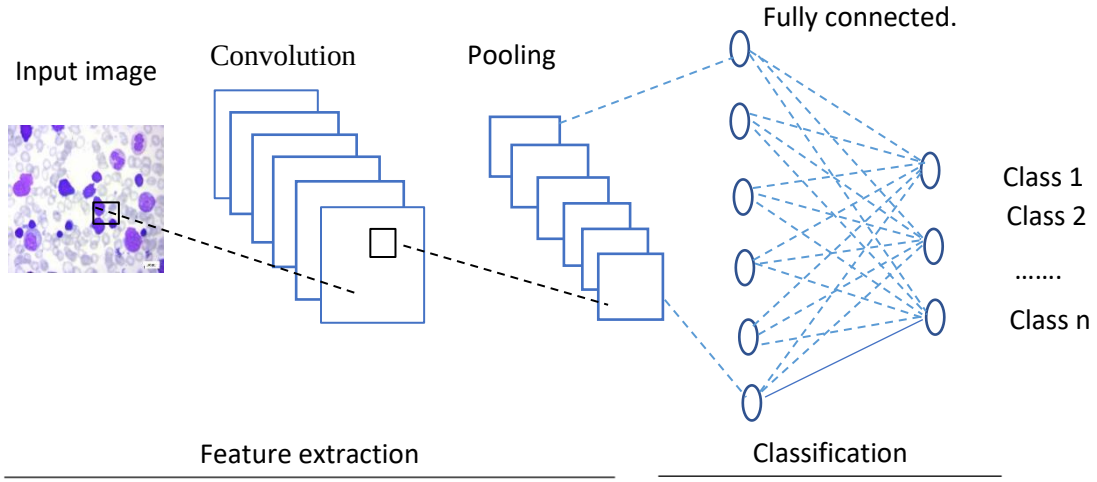

Fig. 1. Convolution neutral network architecture.

II. Related Work

This section presents an overview of previous research conducted on blood cancer classification, focusing on the methods and techniques employed by researchers to accurately identify and classify various types of blood cancer. These studies have made significant contributions to the development of more effective diagnostic tools and have enhanced our understanding of this complex disease.

In [4] Maíla et al. (2022) developed a CNN-based model for the classification of leukemia. They utilized a dataset consisting of 3,536 images from 18 different sources, which were divided into four classes: healthy (1,434 images), ALL (881 images), AML (978 images), and other types (243 images). To enhance the quality of the images, the study employed data augmentation techniques. By applying multilevel and ensemble CNN architectures to the four-class scenario, the researchers achieved accuracy rates of 94.73% and 94.59%.

In [13], Amjad et al. (2018) developed a CAD for the classification ALL subtypes. The dataset utilized in their study consisted of images of ALL subtypes, including 100 images of L1, 100 images of L2, 30 images of L3, and 100 images of normal cells. The proposed system employed segmentation and

deep learning methods, utilizing the AlexNet convolutional neural network architecture. With this approach, an accuracy of 97.78% was achieved.

In [3], Sara et al. (2019) proposed an automated deep learning method utilizing a hybrid approach for distinguishing between immature leukemic blasts and normal cells. The study employed two CNN architectures, namely MobileNet and VGG16. The ISBI 2019 dataset was utilized, consisting of 7,272 images of ALL cells and 3,389 images of healthy cells. The proposed approach achieved an accuracy of 96.17%.

In [6], Nighat et al. (2020) employed the DenseNet-121 and ResNet-34 Convolutional Neural Network architectures for leukemia subtype identification. Both ResNet-34 and DenseNet-121 utilized data augmentation techniques to analyze various image patterns. The study utilized the publicly available ALL-IDB and ASH image bank datasets for leukemia analysis. After augmentation, the dataset consisted of 1,079 images for the ALL class, 1,194 images for the AML class, 840 images for the CLL class, 1,243 images for the CML class, and 1,280 images for the healthy class. The accuracy rate achieved was 99.91% for DenseNet-121 and 99.96% for ResNet-34.

In [11], Maneela et al. (2021) proposed a model for AML detection using the AlexNet and LeNet-5 Convolutional Neural Network architectures. The dataset utilized in this study comprised 4,000 images, with 1,000 images in the lymphocytes class, 1,500 images in the abnormal monocytes class, and 1,500 images in the normal monocytes class. The data was obtained from a hospital in Peshawar, Pakistan. The AlexNet model achieved an accuracy of 98.58%, while the LeNet-5 model achieved an accuracy of 96.25%.

In [1], Arjun et al. (2022) developed a model for leukemia detection utilizing machine learning and deep learning techniques. The study introduced a novel dataset consisting of 500 blood smear images, including images of normal cells, AML cells, and ALL cells. Both binary classification and three-class classification were performed in the study. The proposed approach achieved an accuracy of 97% using VGG16 and 98% using DenseNet121, along with a support vector machine for binary classification. For the three-class classification, an accuracy of 95% was achieved using ResNet50.

In [14], Laura et al. (2021) developed a predictive model for leukemia identification. The dataset used in this study consisted of 16,450 single cells. Various CNN architectures, including VGG16, ResNet101, DenseNet121, and SENet154, were employed to evaluate the model. The best performance was achieved by SENet154 and VGG16, both achieving an accuracy of 94.6%.

In [15], Xiaoli et al. (2021) proposed a deep residual neural network model for the classification of three types of lymphoma: CLL, FL, and MCL. The dataset used in this study consisted of 374 lymphoma pathology images. The model achieved an accuracy of 98.63%.

In [16], Nadia et al. (2019) developed a deep learning model to classify lymphoma subtypes, including CLL, FL, and MCL. The ResNet-34 architecture was utilized to evaluate the model, achieving an accuracy of 95.47%. The dataset used in this study consisted of 374 lymphoma images.

In [17], Hiroaki et al. (2020) proposed an ensemble deep neural network model for classifying three types of lymphoma: FL, diffuse large B-cell lymphoma (DLBCL), and reactive lymphoid hyperplasia (RL). The dataset used in this study consisted of a total of 6,183 images. The model achieved an accuracy of 97%.

III. Proposed Model

The goal of this study is to build a model for blood cancer classification to help doctors and physicians diagnose blood cancer in its early stages and determine treatment to save human lives. This includes three main tasks: data collection, preprocessing, and finally, classification of blood cancer images using CNN architectures. The model is shown in Fig. 2.

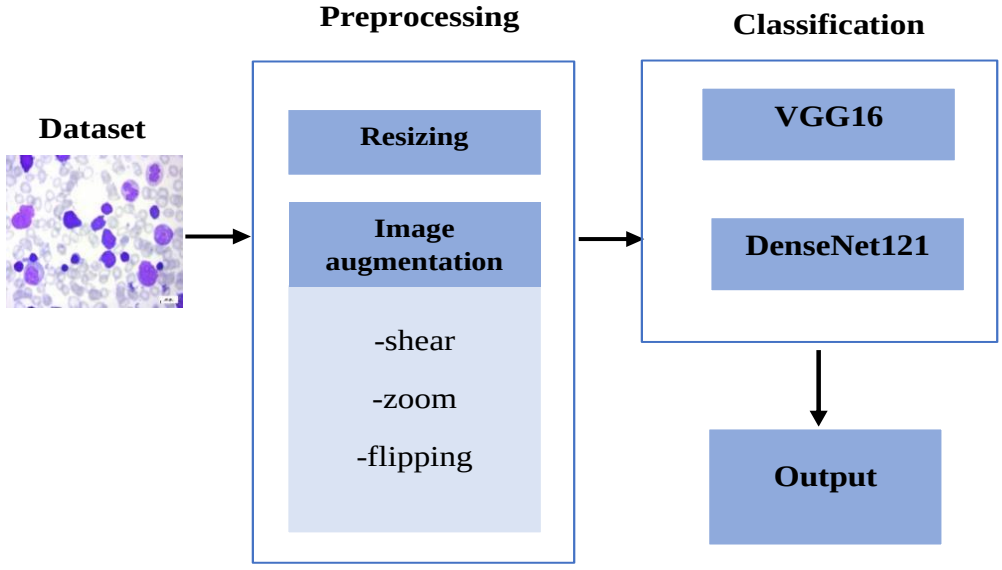

Fig. 2. Proposed model.

A. Dataset

Due to the scarcity of medical data caused by privacy concerns, obtaining sufficient data for biomedical research can be challenging. In this study, we addressed this issue by combining three public datasets [18, 19] to create a larger and more comprehensive dataset for our blood cancer classification model. The dataset consists of 3,679 images across eight different classes. Table I provides a summary of the dataset used.

TABLE I. SUMMARY OF USED DATASET

Class	Number of images	Dataset	Image size
Benign	504	Kaggle	224 ×224
Early ALL	985		224 ×224
Pre-ALL	963		224 ×224
Pro ALL	804		224 ×224
CLL	113		1388 ×1040
FL	139		1388 ×1040
MCL	122		1388 ×1040
AML	49	ASH	960 ×720

B. Preprocessing

We used pre-processing and augmentation techniques to improve the quality of visual information in each input image, thereby enhancing the visibility of essential structures.

1) Resizing: As a result of using multiple datasets with different image sizes, all input images were processed by resizing them to 224×224 to fit the input of our model.

2) Image augmentation: Image augmentation is utilized to train the model. It involves creating modified versions of the dataset images, thereby increasing the size of the training dataset. However, image augmentation serves a dual purpose: not only does it expand the dataset, but it also introduces variability to the data, enabling the model to generalize better to unseen data and address the issue of overfitting. Additionally, as the model is trained in slightly altered images, it becomes more robust and reliable. The preferred method of data augmentation is in-place or on-the-fly augmentation, implemented through Keras' ImageDataGenerator class [20]. This approach exposes the network to diverse variations in the dataset during each epoch of training. By creating additional versions of the original dataset images, the number of images used in each experiment is quadrupled, augmenting the data, and facilitating the classification process.

Before applying any processing, the input is rescaled by a factor known as "rescale." The original RGB coefficients of the images range from 0 to 255, which would be too high for the models to effectively learn at a standard learning rate. Therefore, the original images are rescaled by a factor of 1/255. This rescaling involves multiplying the image data by this value, resulting in image values between 0 and 1. Additionally, three image augmentation techniques are employed: shear, zoom, and flipping.

Shear is one of the image augmentation techniques employed by Keras' ImageDataGenerator, and it utilizes a shear range of 0.2. The shear angle is represented by a floating-point number, indicating the degree of shear in the anticlockwise direction.

The images are also enhanced through zooming. There are two zoom options available: zooming out of the image or zooming in on the image. The ImageDataGenerator class accepts a float value for the zoom range as input. The zoom is applied within the range [1 - zoom range, 1 + zoom range]. Alternatively, instead of providing a float number, a list with two values representing the lower and upper limits can be used [20]. When the value is less than one, the image zooms in, while any value greater than one causes the image to zoom out.

Flipping an image involves reflecting it around its vertical axis, horizontal axis, or both axes simultaneously. This technique allows users to augment the number of images in a dataset without the need for any artificial processing [20]. In this study, random horizontal flipping is used.

C. Classification

Finally, the data was ready for the classification process. The model was trained using two CNN architecture models: VGG16 and DenseNet121. These classification architectures were implemented on Google Collaboratory.

1) DenseNet121: It facilitates the training of deep learning models by solving the vanishing gradient problem, increasing feature reuse, and reducing parameter usage. It has achieved progressive performance in a variety of computer vision tasks [21]. The DenseNet architecture is shown in Fig. 3.

2) VGG16: The VGG-16 network includes 16 convolution layers and a small receptive field of 3×3. It has a Max pooling layer of size 2×2 and 5 such layers in total. After the last Max pooling layer, there are three fully connected layer [22]. A schematic of VGG-16 architecture is illustrated in Fig. 4.

3) Parameters: All the model's parameters are explained, including the activation function, loss function, optimizer, and metrics.

a) Activation function: Another form of activation function applied in neural computing is the softmax function. It estimates the probability distribution from a vector of real numbers. The softmax function returns arrange of values between 0 and 1, with the total of the probability equal to 1[23]. Softmax is shown in Eq. 1. The softmax function is used in multiclass models to produce probabilities for each class.

$$F(y_i) = \frac{e^{(y_i)}}{\sum_j e^{(y_j)}} \quad (1)$$

Where y is input vector.

b) Loss function: The loss function is employed to evaluate the network's effectiveness [24]. The Categorical Cross-Entropy loss, also described as softmax Cross-Entropy loss (CE), is employed in this research. It is employed in multi-class classification. the Categorical Cross-Entropy loss function is showed as in Eq. 2.

$$CE = -\log(\frac{e^{y_a}}{\sum_i^n e^{y_i}}) \quad (2)$$

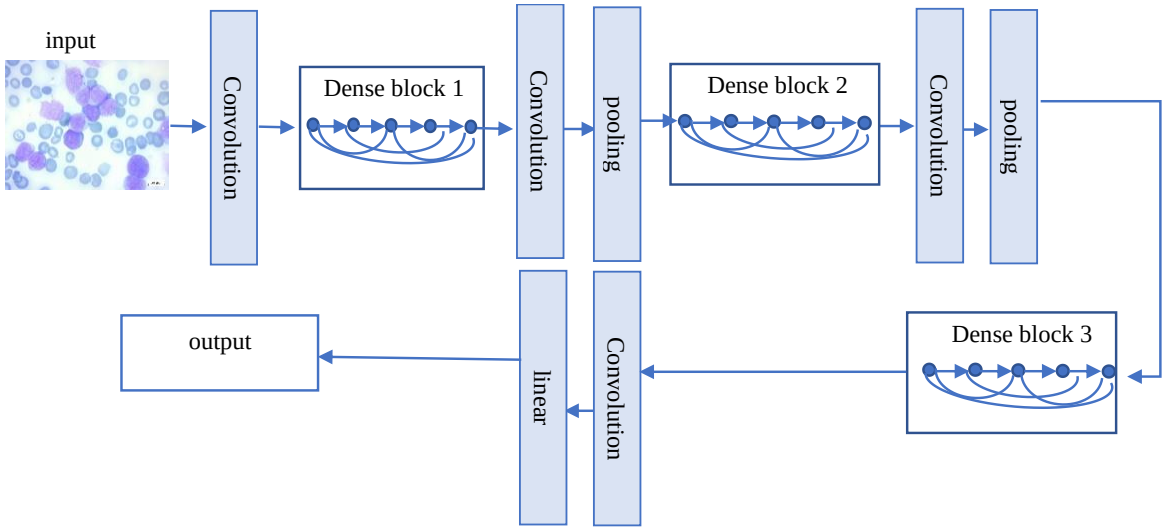

Fig. 3. DenseNet architecture.

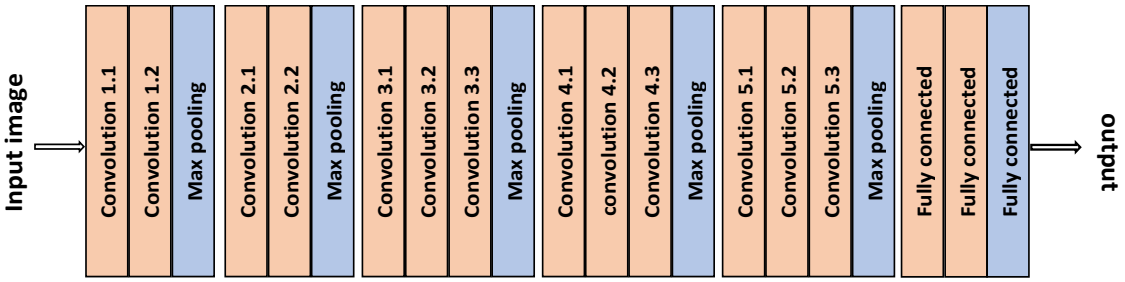

Fig. 4. A schematic of VGG-16 architecture.

Where y_a represents the score for the positive classes in CNN.

c) Optimizer: In the training data, adaptive moment estimation (Adam) is used to correctly update the network weights iteratively. It employs first and second gradient descent computation to fit the learning rate parameter for each weight in the neural network, the first moment represents the mean, and the second represents the uncentered variance, The learning rate is the percentage by which weights are updated; the default learning rate is 0.001. High values accelerate learning before the rate is changed, and lower values slow learning in training [25].

d) Evaluation metrics: The model is evaluated based on accuracy (Acc) metrics; accuracy is a common metric used to evaluate the performance of a classification model. It measures the proportion of correct predictions made by the model compared to the total number of predictions. To calculate accuracy, we typically use a confusion matrix. A confusion matrix is a table that summarizes the performance of a classification model by showing the counts of true positive (TP), true negative (TN), false positive (FP), and false negative (FN) predictions. Each row of the matrix represents the instances in a predicted class, while each column represents the instances in an actual class as shown in Fig. 5. Eq. 3 Illustrates accuracy function.

- True Positive (TP): The model correctly predicted instances as positive when, they were positive. These are the correctly classified positive instances.
- True Negative (TN): The model correctly predicted instances as negative when they were negative. These are the correctly classified negative instances.
- False Positive (FP): The model incorrectly predicted instances as positive when they were negative. These are the instances of the model mistakenly classified as positive.
- False Negative (FN): The model incorrectly predicted instances as negative when they were positive. These are the instances of the model mistakenly classified as negative.

$$\text{Acc} = \frac{TP+TN}{TP+TN+FP+FN} * 100 \quad (3)$$

		Predicted value.	
		positive (P)	Negative (N)
Actual class	P	True positive (TP)	False negative (FN)
	N	False positive (FP)	True negative (TN)

Fig. 5. Confusion matrix.

IV. Result

VGG16 and DenseNet121 CNN architectures were utilized to classify 8 types of blood cancers. The models were trained for 20 epochs with a batch size of 64. The dataset comprised a total of 3,679 images, with 2,733 images allocated for training and 946 images for testing. Fig.6 displays samples of the blood cancer images. The models were evaluated using unseen data to assess their generalization capability. The accuracy of the models was measured, and the results revealed impressive accuracy rates. VGG16 achieved an accuracy of 98.2%, while DenseNet121 achieved an accuracy of 98.1%, as presented in Table II.

The plot diagram when using 20 epochs and DenseNet121 architecture is shown in Fig. 7, plot between train accuracy and validation accuracy is shown in Fig. 7(a), plot between train loss and validation loss is shown in Fig. 7(b). The plot diagram when using 20 epochs and VGG16 architecture is shown in Fig. 8, plot between train loss and validation loss is shown in Fig. 8(a), plot between train accuracy and validation accuracy is shown in Fig. 8(b).

A. Comparison with the State-of-the-Art

In this section a comparison between the proposed model and the state of the art is presented as shown in Table III.

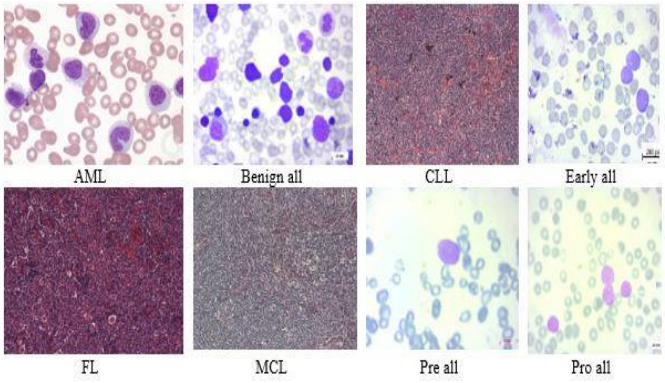

Fig. 6. Samples of the blood cancers images.

TABLE II. Results Obtained by VGG16 and DensNet121 CNN Architectures

Model	#Of epochs	Accuracy	Batch size	Time for each epoch
VGG16	20	98.2%	64	21 s
DensNet121	20	98.1%	64	21 s

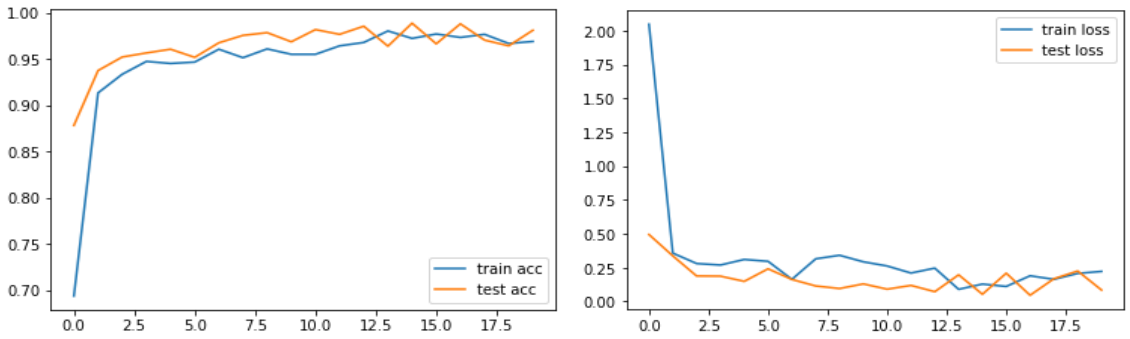

(a) (b)

Fig. 7. The plot diagram when using 20 epochs and DenseNet121 architecture.

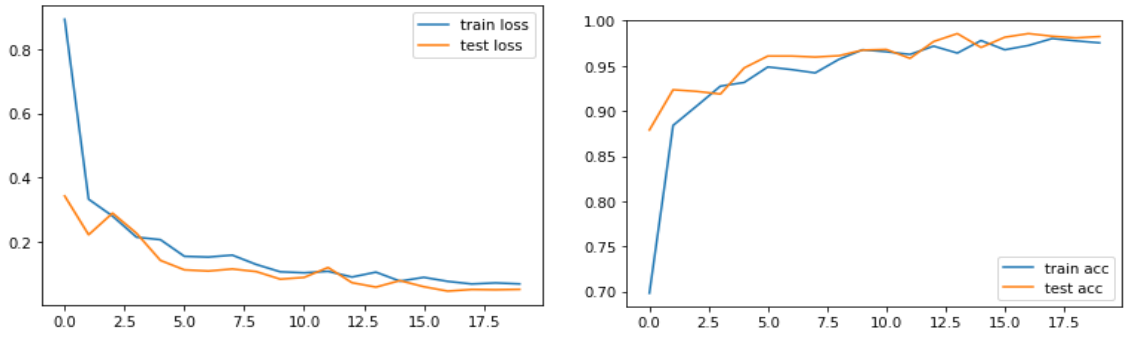

(a) (b)

Fig. 8. The plot diagram when using 20 epochs and VGG16 architecture.

TABLE III. COMPARISON BETWEEN THE PROPOSED MODEL AND THE STATE-OF-THE-ART

#	Research	Year	Model	#Classes	#Images	Accuracy
1	[4]	2022	ensemble CNN architectures	4	3,536	94.73%
2	[13]	2018	Alexnet	4	330	97.78%.
3	[3]	2019	hybrid CNN architectures	2	10,661	96.17%.
4	[6]	2020	DenseNet-121	4	5591	99.91%
5			ResNet-34			99.96%.
6	[11]	2021	AlexNet	3	4000	98.58%
7			LeNet-5			96.25%.
8	[1]	2022	VGG 16	2	500	97%
9			DenseNet121			98%
10			ResNet50	3		95%
12	[15]	2021	residual neural network	3	374	98.63%.
13	[16]	2019	ResNet-34	3	374	95.47%.
14	[17]	2020	ensemble deep neural network	3	6,183	97%.
15	Proposed model	2023	VGG16	8	3,679	98.2%,
			DenseNet121			98.1%.

V. DISCUSSION

This study has made significant progress in the field of blood cancer research by classifying eight different types of blood cancer using deep learning algorithms. Previous studies did not classify these eight types of blood cancer. Two different CNN architectures, namely VGG16 and DenseNet121, were employed for the classification process. The softmax activation function was used to calculate the probabilities of each class, ranging from 0 to 1, based on the CNN outputs. The highest probability corresponds to the predicted class for a given input. The effectiveness of the network was evaluated using the Categorical Cross-Entropy loss function, which measures the dissimilarity between the predicted probabilities and the actual target values, enabling the assessment of model performance. During the training process, the Adam optimizer was used to iteratively update the network's weights. The optimizer aims to find the optimal set of weights that minimize the loss function, thereby improving classification accuracy. The results of the classification process indicate that the VGG16 model achieved the highest accuracy among the two architectures, with a value of 98.2%. This means that the VGG16 model correctly classified 98.2% of the instances in the dataset. On the other hand, the DenseNet121 model achieved a slightly lower accuracy of 98.1%. These accuracy values suggest that both models performed exceptionally well in classifying the eight types of blood cancer, with VGG16 demonstrating slightly better performance compared to DenseNet121.However, the study encountered several challenges. Acquiring sufficient high-quality data proved to be a major hurdle as blood cancer datasets were often limited in size and lacked diversity, posing challenges in developing a robust and accurate model. Ensuring data accuracy and reliability was crucial for obtaining meaningful results. Another significant challenge was the interpretability and explainability of deep learning models. In the context of medical research, interpretability is vital for gaining insights into the underlying factors contributing to the classification. Developing methods to explain the model's predictions and provide interpretable results was a significant undertaking. Furthermore, the study required substantial computational resources and time to train complex models on large datasets. Access to high-performance GPUs and collaboration with medical experts were essential for effective model training and evaluation. Bridging the gap between deep learning expertise and domain-specific knowledge posed additional challenges, emphasizing the need for collaboration with experts in blood cancer pathology, diagnosis, and treatment. Addressing these challenges was crucial in developing an accurate and reliable blood cancer classification model that aligns with clinical practices and aids in advancing diagnosis and treatment strategies.

VI. CONCULSION

This work presents the classification of blood cancer types using state-of-the-art deep learning techniques. Leukemia and lymphoma are hematological diseases and types of blood cancer that cause abnormal behavior in blood cells. In this study, we propose VGG16 and DenseNet121-based models to classify two types of leukemia and three subtypes of lymphoma and compare their performance. Data augmentation techniques are also employed to address the issue of overfitting, resulting in improved results. The proposed models are evaluated using unseen images that were not included in the training phase. The VGG16 architecture achieves the highest accuracy of 98.2%, while DenseNet121 exhibits slightly lower accuracy.

In future work, we plan to expand the classification to include other types of blood cancer, such as myeloma and chronic myeloid leukemia. Additionally, we aim to evaluate the proposed dataset using various deep learning algorithms to compare their performance in this field of research. Furthermore, an online Internet of Things (IoT) application will be developed to collect and analyze a larger volume of blood data.

REFERENCES

[1] Abhishek, A., et al., Automated classification of acute leukemia on a heterogeneous dataset using machine learning and deep learning techniques. Biomedical Signal Processing and Control, 2022. 72: p. 103341.

[2] McCabe, B., F. Liberante, and K.I. Mills, Repurposing medicinal compounds for blood cancer treatment. Annals of hematology, 2015. 94(8): p. 1267-1276.

[3] Kassani, S.H., et al. A hybrid deep learning architecture for leukemic B-lymphoblast classification. in 2019 International Conference on Information and Communication Technology Convergence (ICTC). 2019. IEEE.

[4] Claro, M.L., et al., Assessing the impact of data augmentation and a combination of CNNs on leukemia classification. Information sciences, 2022. 609: p. 1010-1029.

[5] Raina, R., et al., A Systematic Review on Acute Leukemia Detection Using Deep Learning Techniques. Archives of Computational Methods in Engineering, 2022: p. 1-20.

[6] Bibi, N., et al., IoMT-based automated detection and classification of leukemia using deep learning. Journal of healthcare engineering, 2020. 2020.

[7] Shafique, S. and S. Tehsin, Acute lymphoblastic leukemia detection and classification of its subtypes using pretrained deep convolutional neural networks. Technology in cancer research & treatment, 2018. 17: p. 1533033818802789.

[8] Ghaderzadeh, M., et al., A fast and efficient CNN model for B-ALL diagnosis and its subtypes classification using peripheral blood smear images. International Journal of Intelligent Systems, 2022. 37(8): p. 5113-5133.

[9] Reena, M.R. and P. Ameer, A content-based image retrieval system for the diagnosis of lymphoma using blood micrographs: An incorporation of deep learning with a traditional learning approach. Computers in Biology and Medicine, 2022. 145: p. 105463.

[10] El Achi, H., et al., Automated diagnosis of lymphoma with digital pathology images using deep learning. Annals of Clinical & Laboratory Science, 2019. 49(2): p. 153-160.

[11] Shaheen, M., et al., Acute myeloid leukemia (AML) detection using AlexNet model. Complexity, 2021. 2021.

[12] Rachapudi, V. and G. Lavanya Devi, Improved convolutional neural network based histopathological image classification. Evolutionary Intelligence, 2021. 14(3): p. 1337-1343.

[13] Rehman, A., et al., Classification of acute lymphoblastic leukemia using deep learning. Microscopy Research and Technique, 2018. 81(11): p. 1310-1317.

[14] Boldú, L., et al., A deep learning model (ALNet) for the diagnosis of acute leukaemia lineage using peripheral blood cell images. Computer Methods and Programs in Biomedicine, 2021. 202: p. 105999.

[15] Zhang, X., et al., Research on the classification of lymphoma pathological images based on deep residual neural network. Technology and Health Care, 2021. 29(S1): p. 335-344.

[16] Brancati, N., et al., A deep learning approach for breast invasive ductal carcinoma detection and lymphoma multi-classification in histological images. IEEE Access, 2019. 7: p. 44709-44720.

[17] Miyoshi, H., et al., Deep learning shows the capability of high-level computer-aided diagnosis in malignant lymphoma. Laboratory Investigation, 2020. 100(10): p. 1300-1310.

[18] Orlov, N.V., et al., Automatic classification of lymphoma images with transform-based global features. IEEE Transactions on Information Technology in Biomedicine, 2010. 14(4): p. 1003-1013.

[19] Aria, M., et al., Acute lymphoblastic leukemia (all) image dataset. Kaggle, 2021.

[20] Khalifa, N.E., M. Loey, and S. Mirjalili, A comprehensive survey of recent trends in deep learning for digital images augmentation. Artificial Intelligence Review, 2022. 55(3): p. 2351-2377.

[21] Sarker, L., et al., COVID-DenseNet: a deep learning architecture to detect COVID-19 from chest radiology images. Preprint, 2020. 2020050151.

[22] Theckedath, D. and R. Sedamkar, Detecting affect states using VGG16, ResNet50 and SE-ResNet50 networks. SN Computer Science, 2020. 1(2): p. 1-7.

[23] Nwankpa, C., et al., Activation functions: Comparison of trends in practice and research for deep learning. arXiv preprint arXiv:1811.03378, 2018.

[24] Wang, Q., et al., A comprehensive survey of loss functions in machine learning. Annals of Data Science, 2022. 9(2): p. 187-212.

[25] Kingma, D.P. and J. Ba, Adam: A method for stochastic optimization. arXiv preprint arXiv:1412.6980, 2014.